Journal of the Endocrine Society, 2022, **6**, 1–9
https://doi.org/10.1210/jendso/bvac076
Advance access publication 10 May 2022
Clinical Research Article

Papillary Thyroid Cancer and a *TERT* Promotor Mutation-positive Paraganglioma in a Patient With a Germline *SDHB* Mutation

Ali S. Alzahrani,[1,2] Meshael Alswailem,[1,*] Avaniyapuram Kannan Murugan,[1,*] Balgees Alghamdi,[1] and Hindi Al-Hindi[3]

[1]Department of Molecular Oncology, King Faisal Specialist Hospital & Research Centre, Riyadh, 11211, Saudi Arabia
[2]Department of Medicine, King Faisal Specialist Hospital & Research Centre, Riyadh, 11211, Saudi Arabia
[3]Department of Pathology and Laboratory Medicine, King Faisal Specialist Hospital & Research Centre, Riyadh, 11211, Saudi Arabia

*M.A. and A.K.M. contributed equally to this work.
Correspondence: Ali S. Alzahrani, MD, MBC-46, P.O. Box 3354, Department of Medicine, King Faisal Specialist Hospital & Research Centre, Riyadh, 11211, Saudi Arabia. Email: aliz@kfshrc.edu.sa

Abstract

Purpose: About 40% of paragangliomas (PGL) are due to germline mutations in one of several susceptibility genes. These genes rarely predispose to other non-PGL tumors. Here, we describe and functionally characterize a germline *SDHB* mutation in a patient who developed a $BRAF^{V600E}$ mutation-positive papillary thyroid cancer (PTC) and a *TERT* promotor mutation-positive PGL.

Experimental design: A 28-year-old asymptomatic man was discovered incidentally to have a large left-sided mid-abdominal PGL and PTC. He underwent resection of the PGL and total thyroidectomy and neck dissection followed by I-131 adjuvant therapy for PTC. The histopathology revealed a high-grade PGL and a tall cell-variant PTC with lymph node metastases (T1b N1b M0). He soon developed PGL spinal metastases that have been rapidly progressing and is currently being treated with Lu^{177}-dotatate therapy. Family screening revealed a positive *SDHB* mutation in the mother, a son, and a brother.

Results: In addition to the heterozygous *SDHB* germline mutation (c.688C>T, p.Arg230Cys), molecular analysis revealed a somatic *TERT* promotor mutation (C228T) in PGL (negative in PTC) and a somatic $BRAF^{V600E}$ mutation in PTC (negative in PGL). Functional studies showed a higher proliferation rate in the mutant compared with the wild-type SDHB.

Conclusion: Germline *SDHB* mutations rarely occur in patients with PTC and may contribute to its aggressiveness. Somatic *TERT* promotor mutations rarely occur in PGL and contribute to its aggressiveness and metastatic potential.

Key Words: papillary thyroid cancer, paraganglioma, SDHB, TERT, BRAF, mutations

Abbreviations: CS, Cowden syndrome; CSL, Cowden syndrome-like; CT, computed tomography; FDG, F-18-fluorodeoxyglucose; MRI, magnetic resonance imaging; PCC, pheochromocytoma; PET, positron emission tomography; PGL, paraganglioma; PPGL, paraganglioma and pheochromocytoma; PTC, papillary thyroid cancer; *SDHx*, succinate dehydrogenase group; TCGA, The Cancer Genome Atlas; *TERT*, telomerase reverse transcriptase

Paraganglioma (PGL) and pheochromocytoma (PCC), together abbreviated as PPGL, are neuroendocrine chromaffin cell-derived tumors [1, 2]. PCC arises from the adrenal medulla and PGL arises from the ganglia of the autonomic nervous system [2]. The most common locations for PGL are the head and neck area and the retroperitoneum in the abdomen, but PGL occurs in the mediastinum, pelvis, and sometimes in the urinary bladder, lungs, and anterior abdomen [1, 3]. Over the past 2 decades, it has become clear that about 40% of PPGL are familial/hereditary [4, 5]. More than a dozen predisposing genes have been identified [2, 4]. The most commonly mutated genes are the succinate dehydrogenase group (*SDHx*) that includes *SDHA*, *SDHB*, *SDHC*, *SDHD*, and *SDHAF2* [4–6]. Other, less-frequently reported predisposing genes include *FH*, *MAX*, *RET*, *MDH2*, *VHL*, *NF1*, and *TMEM127* [2, 6, 7]. Although most PPGL are benign, about 10% to 40% are metastatic [8]. The risk of metastases correlates with the underlying genetic mutations [7, 8]. The clearest association between the risk of distant metastases and the underlying gene mutations is with *SDHB* [9, 10]. Patients carrying mutations in this gene have about 40% risk of developing distant metastases and are at an increased risk of death from PGL [9, 10].

Papillary thyroid cancer (PTC) is the most common endocrine malignancy [11]. Overall, its prognosis is excellent [12, 13]. However, about 20% to 25% of cases are aggressive tumors and associated with a high risk of recurrence and mortality [14, 15]. Factors associated with increased risk of recurrence and mortality include the size of the tumor, histopathological subtype, vascular invasion, gross extrathyroidal extension, and lymph node and distant metastases [13]. Many somatic mutations have also been associated with the risk of recurrence and mortality from PTC [16, 17]. The most common genetic alteration is the $BRAF^{V600E}$ mutation occurring in about 60% of PTC [16]. This mutation has been associated with more aggressive histopathological features

Received: 1 March 2022. **Editorial Decision:** 3 May 2022. **Corrected and Typeset:** 3 June 2022

and higher risk of recurrence and mortality [18–20]. Another relatively recently discovered genetic alteration is mutations in the telomerase reverse transcriptase (*TERT*) promotor region. *TERT* promotor mutations are associated with more aggressive histopathological features and high risk of metastasis, recurrence, and mortality [21, 22]. $BRAF^{V600E}$ and *TERT* mutations, when they occur together in the same tumor, are associated with the highest risk of recurrence and mortality [23].

The occurrence of PGL and PTC in the same patient is extremely rare and their association is not clear. In this report, we describe an interesting case of a young man who was found to have a large abdominal PGL and PTC. Genetic testing revealed a germline *SDHB* mutation (p.Arg230Cys). Molecular profiling of his PGL and PTC revealed a *TERT* promotor mutation (C228T) in the PGL and $BRAF^{V600E}$ in PTC. Although *TERT* promotor mutations are more typically found in PTC [24, 25], it was negative in this case in the PTC but positive in the PGL. The course of the disease in this patient is characterized by a very aggressive metastatic PGL. This is most likely related to the underlying germline *SDHB* mutation and the somatic *TERT* promotor mutation. The interplay and synergy between these different genetic alterations are the subject of this paper.

Patients and Methods

AA is a 28-year-old man who complained of a left scrotal swelling, which was diagnosed as a varicocele in September 2019. During a workup for that complaint, a computed tomography scan (CT) and magnetic resonance imaging (MRI) showed a large left midline abdominal mass measuring 6.4 × 7.9 × 11.8 cm (Fig. 1A). It was compressing the left ureter causing moderate hydroureteronephrosis. Laparoscopic biopsy of the mass showed a neuroendocrine tumor consistent with PGL. The patient was completely asymptomatic at that time. Specifically, he had no palpitations, sweating or headache, anxiety, panic attacks, tremors, heat or cold intolerance, fatigue, weight loss, or loss of appetite. He was exercising regularly with excellent stamina. No history of abdominal pain or changes of bowel habits and no history of hypertension. His family history was negative for PPGL, Von Hippel-Lindau syndrome, neurofibromatosis, other types of cancer, or rare syndromes. One brother has sickle cell disease and 3 other brothers have sickle cell trait. The father has end-stage renal disease of an unclear cause and had renal transplants twice with a good functioning graft. The mother reported no symptoms or significant illness.

Laboratory investigations showed normal 24-hour urine metanephrines (repeated 3 times) normetanephrine 1.54 µmol/L (0-3.43), metanephrine 0.78 µmol/L (0-1.49), and 3-methoxytyramine 1.02 µmol/L (0-2.06). An F-18-fluorodeoxyglucose positron emission tomography/computed tomography (FDG PET CT) scan showed an intense uptake in the abdominal PGL without other foci in the abdomen, lungs, or skeleton, but there was a left thyroid PET incidentaloma (Fig. 1B and 1D). An ultrasound of the thyroid gland showed a solid hypoechoic left mid-thyroid lobe nodule measuring 1.2 × 0.9 × 0.8 cm with tiny foci of punctate calcifications and multiple prominent left supraclavicular lymph nodes, the largest of which measured 0.3 cm (Fig. 1C). Fine-needle aspiration biopsy from thyroid nodule confirmed the diagnosis of PTC.

In February 2020, the patient was prepared with phenoxybenzamine 10 mg 3 times daily for 2 weeks and underwent tumor embolization followed by resection of the left retroperitoneal mass, with resection/anastomosis of part of lower descending colon and resection of a small part of the left ureter. The histopathological examination showed an 11-cm PGL with small and large vascular invasion, capsular invasion, involvement of resection margin by the tumor, and adventitial ureteric invasion. The tumor has several features that are associated with aggressive behavior including a large size, vascular and capsular invasion, architectural and cytological atypia, and high mitotic activity. The Ki67 index was also high at 40%. Immunohistochemistry showed the following: synaptophysin: positive; chromogranin: positive; GATA-3, positive; and S100: positive in sustentacular cells. The patient had an uneventful postoperative recovery.

In August 2020, the patient underwent total thyroidectomy and bilateral central and left lateral neck dissection for PTC. Histopathological examination revealed a tall cell variant PTC, bilateral and multifocal, largest focus 1.5 cm with no identifiable vascular invasion, and only minimal perithyroidal

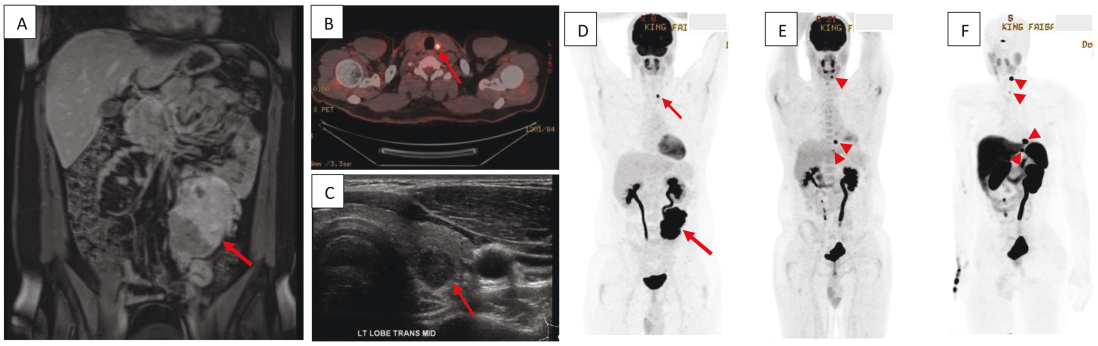

Figure 1. (A) Gadolinium-enhanced coronal T1 MRI image of the abdomen showing a large lobulated heterogeneously enhancing mass with areas of necrosis in the left lower abdomen (arrow). (B) A cross-sectional image of an FDG PET CT scan showing a left thyroid lobe focal lesion (arrow). (C) A horizontal view of the thyroid gland showing a 1.2-cm hypoechoic suspicious nodule corresponding to the PET scan lesion (arrow). (D) A whole-body coronal section of FDG PET scan showing an FDG-avid large left lower and mid-abdomen mass (arrow) corresponding to the mass seen on MRI and the left thyroid lobe incidentaloma (arrow). (E) A follow-up FDG PET CT scan done 1 year after the scan in panel D, showing complete removal of the abdominal PGL and thyroid cancer but the new appearance of spinal metastases at C4 vertebra, left 9th costovertebral junction, and T-10 vertebra (arrowheads). (F) A gallium-68 PET CT whole-body scan done at the same time of FDG PET CT scan shown in panel E showing the same lesions (arrowheads).

extension. There were 11 of 16 central lymph nodes involved by PTC with extranodal extension in some. There were also 3 of 25 left lateral lymph nodes involved with the tumor. The 8th American Joint Committee on Cancer TNM stage was stage I (T1b N1b M0).

In December 2020, after L-thyroxine withdrawal for 4 weeks, he received 109 mCi adjuvant I-131 therapy. The pre- and posttherapy whole-body scans showed foci of uptake of 3.1% in the thyroid bed only with no additional foci outside the neck. Stimulated thyroglobulin at that time was 20.7 µg/L, antithyroglobulin antibodies were negative and TSH was 243 mU/L. In November 2020, a gallium-68 PET CT whole-body scan revealed 2 new foci of uptake in the pedicle of the thoracic spine 8 (T8) and the transverse process of the cervical spine 4 (C4) that were suspicious for metastasis. A whole-spine MRI at that time did not find any corresponding abnormalities in the thoracic or cervical spine and the whole spine was normal. However, a whole-spine MRI in April 2021 showed further progression with left 9th costovertebral junction-altered MRI signal with surrounding soft-tissue thickening and interval development of T10 vertebral body lesion concerning for metastasis. A repeat gallium-68 and FDG PET CT whole body scans showed showed new foci of increased tracer uptake increased tracer uptake at T10 and C7/T1 vertebrae, which were highly suspicious for new bony metastases and progressive tracer avid lesions in the ninth left costovertebral junction/paravertebral region, which could represent a bone metastasis. There was also a progressive tracer avid lesion in the left C4/C5 vertebra bony metastatic lesions (Fig. 1E and 1F). The overall findings confirmed disease progression. The patient is currently stable receiving Lu177 Dotatate radiation therapy for his metastatic PGL. His family members are being evaluated.

Molecular Studies

After obtaining an institutional review board approval and informed consents from the patient and his family members, we isolated DNA from peripheral leucocytes using QIAamp DNA Blood Mini Kit (cat. no. 51104, QIAGEN GmbH - Germany), and from PGL and PTC tissue using QIAamp DNA FFPE Tissue Kit (cat. no. 56404, QIAGEN). All exons and exon-intron boundaries of the *SDHB* gene were initially amplified in the peripheral DNA using primers and amplification conditions as previously described [26]. Subsequently, we amplified and sequenced exon 7 looking for the same mutation in PGL and PTC tumor tissue. We then amplified and sequenced DNA from the peripheral blood, PTC and PGL tissue for $BRAF^{V600E}$, and *TERT* promotor mutations (C228T and C250T) using previously described primers and PCR conditions [27, 28]. We also screened his family, as shown in Fig. 2.

Mammalian Expression Vector, Site-Directed Mutagenesis, and Sequencing

Carboxyl-terminal (C) Myc-DDK-tagged mammalian expression vector carrying a wild-type SDHB (NM_003000) clone (cat. no: RC203182) was purchased from OriGene Technologies, Inc. (Rockville, MD, USA). The SDHB mutant construct was made using the wild-type SDHB-Myc-DDK-tagged plasmid as a template. To create the SDHB R230C mutant, the mutagenesis reaction was performed in a 50-µL reaction using the QuickChange XL-II site-directed mutagenesis kit as recommended by the manufacturer (Agilent Technologies, USA). The molecular size of the plasmids (mutant clones) was checked by ethidium bromide-stained 1% agarose gel in a standard electrophoresis system and mutated nucleotides were confirmed by sequencing (Sanger) using exon 7 primers with 5′ M13 tag (SDHB-F ex.7: GTA AAA CGA CGG CCA GT TCT GCC AAT CAC CTC TTT GTG; SDHB-R ex.7: CAG GAA ACA GCT ATG ACC TGA ATT CCC TTT CCT CTG CAC) by BigDye Terminator v3.1 Cycle Sequencing Kit (ThermoFisher, MA USA).

Plasmid Purification, Mammalian Cell Culture, and Transfection

All the plasmid constructs including C-terminal Myc-DDK-tagged vector, wild-type, and mutant *SDHB* were purified using

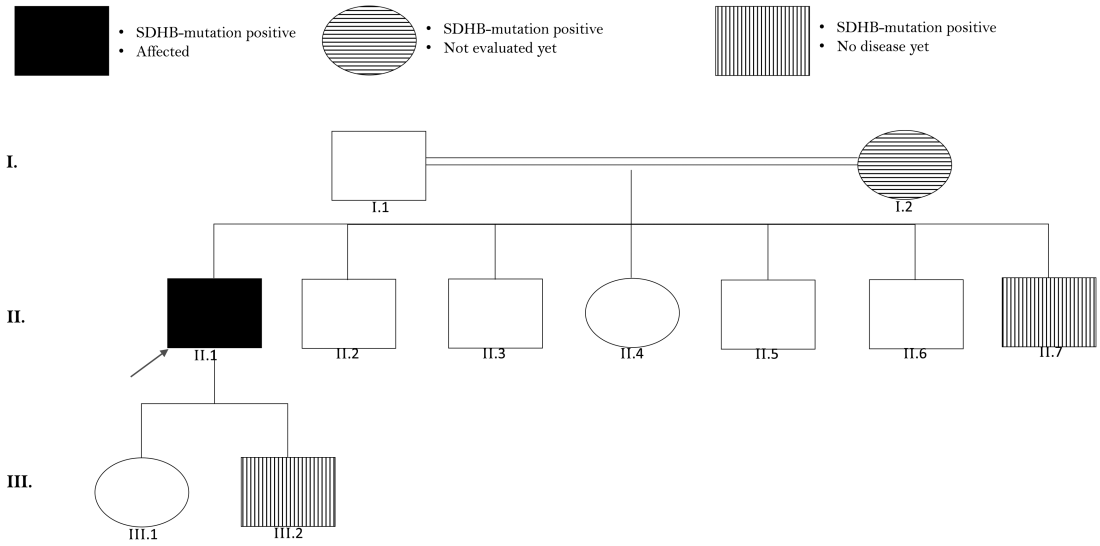

Figure 2. The family pedigree shows affected and unaffected family members. All members were tested for the *SDHB* mutation (p.Arg230Cys). Some of the mutation-positive individuals were evaluated for the presence of disease and some have not yet been tested.

EndoFree plasmid preparation kit as per the manufacturer's instruction (Invitrogen, MA). In our experiments, we used HEK293T (CRL-3216) cells that were purchased from American Type Culture Collection (Manassas, VA, USA) and Nthy-ori 3-1 cells that are an immortalized thyroid follicular epithelial cell line derived from normal adult thyroid tissue (a gift from Dr. Yufei Shi). The cells were cultured and maintained in DMEM with 10% fetal bovine serum, antibiotic, and antimycotic per American Type Culture Collection. One day before the transfection, the HEK293T cells and the Nthy-ori 3-1 cells were plated in 24-well plates. The next day, after cells reached 90% confluence, we transfected these cells with equal amounts of vector, wild-type, and mutant *SDHB* expression constructs using Lipofectamine 2000 (Invitrogen, Carlsbad, CA, USA) as per the manufacturer's recommendation.

Determination of pH

The pH of the cell culture medium collected from the vector, wild-type, and mutant *SDHB* (R230C) transfected HEK293T and Nthy-ori 3-1 cell culture was determined as mentioned previously [29]. Briefly, HEK293T and Nthy-ori 3-1 cells were transfected with equal amounts of each vector, wild-type, and mutant SDHB (R230C) construct as indicated earlier (24-well plate) and 24 hours after transfection, the cell culture medium was replaced with a fresh medium and further incubated for 24 hours. Forty-eight hours after transfection, we collected the culture medium, photographed, and determined the pH at room temperature by SevenCompact pH/Ion S220 (Mettler-Toledo, Zchwerzenbach, Switzerland).

Cell Lysate Preparation and Western Blotting

After collecting the cell culture medium at 48 hours posttransfection for the pH determination, the HEK293T and Nthy-ori 3-1 cells were washed once with ice-cold PBS and lysed on ice using ice-cold radioimmunoprecipitation assay buffer (Sigma-Aldrich). The adherent cells were scraped with a cell scraper, incubated on ice for 45 minutes, and gently transferred into precooled microfuge tubes and centrifuged at 12 000 rpm for 15 minutes at 4°C. Supernatants from the lysed cells were collected in precooled microfuge tubes and were subjected to Western blotting to determine the protein expression of various transfected constructs (vector, wild-type, and mutant SDHB). We used primary antibodies anti-myc (cat. no. sc-40, RRID:AB_627268, https://scicrunch.org/resolver/AB_627268) to detect myc-tagged SDHB and anti-β-actin (cat. no. sc-1616R, RRID:AB_630836, https://scicrunch.org/resolver/AB_630836) for loading control in the Western blotting and was performed as earlier mentioned [30].

Cell Proliferation Assay

The proliferation of cells was measured as described previously [31]. In brief, at 24 hours, HEK293T and Nthy-ori 3-1 cells transiently transfected with vector, wild-type, mutant SDHB (R230C) were washed once with PBS, trypsinized, and seeded at a concentration of 4×10^3 cells/well in 100 µL DMEM with 10% fetal bovine serum in a 96-well tissue culture microplate (Costar, cat. no. 3596, Corning Inc., NY) in triplicate and cells were maintained in standard conditions. Cell proliferation assay was conducted by using the reagent WST-1 (cat. no. 05015944001, Roche), 10 µL/well, and incubated at 37°C with 5% CO_2 for 4 hours. The absorbance of samples was measured against a blank and absorption at 440 nm by a microplate reader (xMark Microplate Spectrophotometer, Bio-Rad).

Wound-healing Assay

Wound-healing assay was performed as mentioned previously [32]. Briefly, HEK293T and Nthy-ori 3-1 cells were transiently transfected with vector, wild-type, and mutant SDHB (R230C) constructs. After 24 hours of transfection, cells were trypsinized and an equal number of cells was plated with higher density (2×10^5 cells/well) in 24-well plates. After 6 hours, a scratch (0.6 mm) was made using a pipette tip on the attached monolayer cells. The cell surface was washed 3 times with PBS and maintained at standard cell culture conditions. As indicated for HEK293T cells, we also performed the wound-healing assay in Nthy-Ori 3-1 cells with a scratch of 1.2 mm. Wound closure was carefully watched at 0 and 24 hours from the initial scratch and photographed at ×20 magnification under the microscope (OPTIKA XDS-3FL4, Italy).

LIMBO Score Determination

LIMBO score indicates the changes in the chaperone binding efficiency of the protein. LIMBO score and the indicated structure for the wild-type and mutant SDHB were derived from the SNPeffect database (https://snpeffect.switchlab.org/). The variant identification number for this SDHB R230C is VAR_054383.

The Cancer Genome Atlas Data Analysis

We analyzed 184 cases of PGL and PCC and 496 cases of papillary thyroid cancer from The Cancer Genome Atlas (TCGA). All the data were analyzed and visualized as described previously [33].

Statistical Methods

All the statistical analyses were performed using GraphPad Prism v.8 (GraphPad Software, CA, USA) and the continuous data were analyzed with unpaired Student *t* test. *P* value < 0.05 was determined as statistically significant. The statistical significance levels between the 2 compared groups are indicated by the asterisk marks ($*P \le 0.05$; $**P \le 0.01$; $***P \le 0.001$; $****P \le 0.0001$).

Results

Germline and Somatic Mutations

Amplification and sequencing of DNA from peripheral blood revealed a previously reported heterozygous *SDHB* mutation (c.688C>T, p.R230C) (Fig. 3). The $BRAF^{V600E}$ mutation was positive in PTC but negative in PGL (Fig. 3). Unexpectedly, the C228T *TERT* promotor mutation was detected in PGL and not in PTC (Fig. 3). $BARF^{V600E}$ and *TERT* promotor mutations were negative in the peripheral blood (Fig. 3). Family screening for the same *SDHB* mutation revealed that the patient's mother, a 17-year-old brother, and a 4-year-old son were positive (Fig. 2). The mother has not yet been evaluated, but the 17-year-old brother and the 4-year old son have been evaluated and so far have no evidence of the disease.

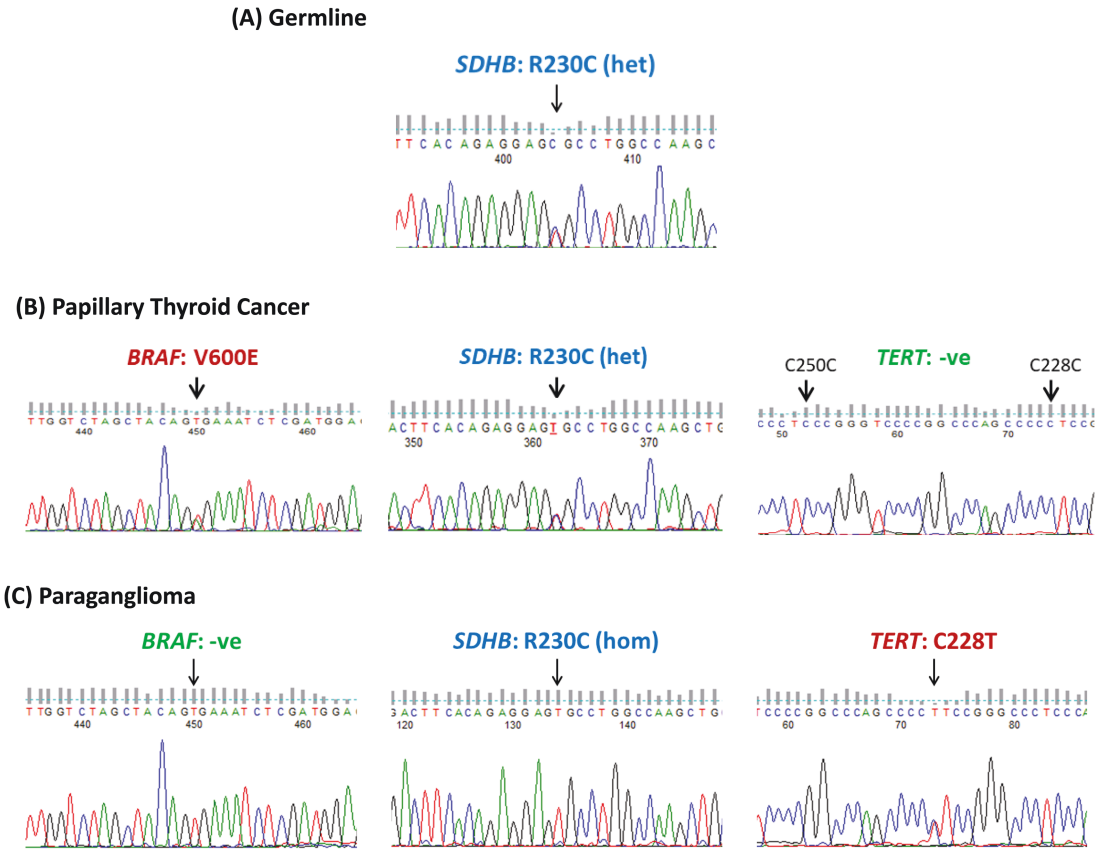

Figure 3. Identification of the germline *SDHB* mutation and the somatic *TERT and BRAF* mutations. The upper panel (leukocyte DNA) shows the heterozygous germline *SDHB* (c.688C>T p.Arg230Cys) mutation. The middle panel (papillary thyroid cancer) shows $BRAF^{V600E}$ mutation (left), a somatic *SDHB* (p.Arg230Cys) mutation (middle), and a negative *TERT* promotor mutation (right). The lower panel (paraganglioma) shows a wild-type *BRAF* (left), a homozygous *SDHB* (p.Arg230Cys) mutation (middle), and C228T *TERT* promotor mutation (right). All the indicated gene sequences in these panels are sense-stranded and repeated 3 times with forward and reverse primers by independent PCR.

Functional Characterization of *SDHB* (p.Arg230Cys) Mutation

HEK293T and Nthy-ori 3-1 cells were transiently transfected with Myc-tagged vector, wild-type, and mutant *SDHB*. Cell lysates from these expression constructs were subjected to Western blotting analyses to ensure success of transfection. After 24 hours, pH was measured and showed a lower pH in the mutant culture medium compared with wild-type and vector alone. The proliferation index was highest in the mutant followed by wild-type and vector alone and the wound healing was most impressive in the mutant construct compared with the wild-type or vector alone. These experiments were repeated 3 times and showed the same results indicating the high oncogenic effect of the p.Arg230Cys mutation (Figs. 4 and 5).

Analyses of the TCGA Data for *SDHB* and *TERT* in PGL and *SDHB* and *BRAF* in PTC

As shown in Fig. 6, somatic *SDHB* mutations were not reported in the 496 well-differentiated PTC TCGA database. Similarly, *TERT* promotor mutations were not reported in the 184 pheochromocytoma and PGL TCGA.

Discussion

In this report, we describe a young man who was found to have an asymptomatic large abdominal PGL during evaluation of a varicocele. During the evaluation of the PGL, he was also found to have a PTC. More interestingly is the molecular genetics of his 2 tumors. He had a previously described germline missense *SDHB* mutation (pArg230Cys), which is the underlying cause for the PGL. Molecular profiling of the PTC unsurprisingly revealed the somatic $BRAF^{V600E}$ mutation. C288T *TERT* promotor mutation that is more characteristic of PTC was not detected in the PTC, but unexpectedly was positive in the PGL. Functional characterization of the p.Arg230Cys *SDHB* mutation confirmed its pathogenicity. Its role in the pathogenesis of PGL is well known [9, 34]. Its pathogenicity in PTC in this patient is suggested by the functional studies that showed an aggressive proliferation and wound healing of the mutant compared to the wild-type *SDHB*. The interactions between these several germline and somatic mutations and their effects on the pathology and course of these tumors are intriguing. PTC in this patient was of an intermediate to high risk with multifocal tall cell variant and several positive central and lateral metastatic lymph nodes, some with extranodal extension (T1b N1b M0). The PGL soon metastasized to the spine, and these metastases were progressive over a short time. It is likely that the $BRAF^{V600E}$ mutation was a strong driver for PTC in this patient and the germline *SDHB* mutation mutation may have contributed to the development and aggressiveness of PTC. The *SDHB* germline mutation (p.Arg230Cys) was the underlying genetic cause for PGL and is well known to be associated with increased risk of metastasis, but the presence

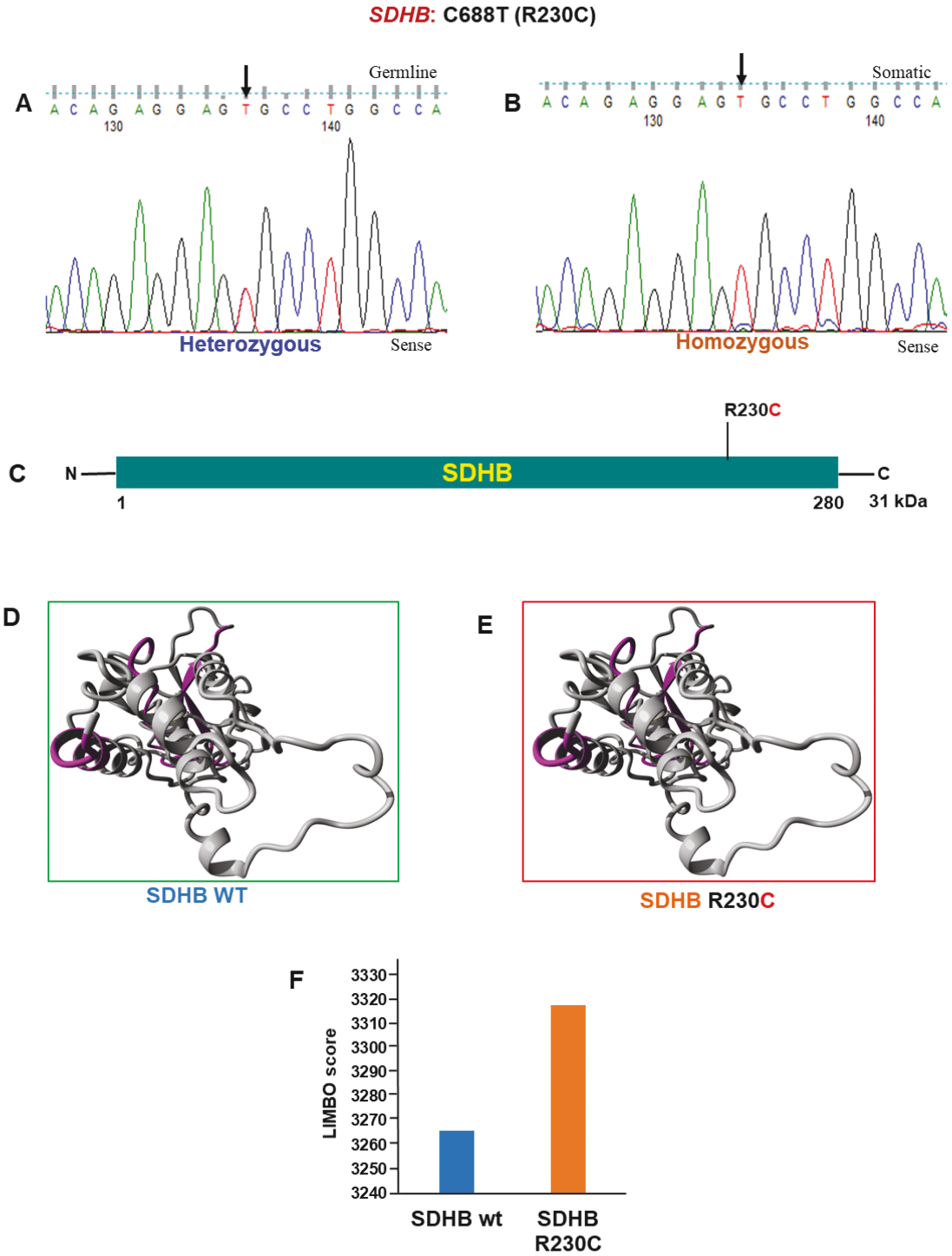

Figure 4. Identification of *SDHB* mutation in paraganglioma. (A) Chromatopherogram shows the germline heterozygous mutation of *SDHB* gene in exon 7 at coding nucleotide position 688 changing C to T nucleotide resulting in p.Arg230Cys. (B) Chromatopherogram shows loss of heterozygosity (a homozygous c.688C>T *SDHB* mutation. (C) A Schematic diagram shows the SDHB protein and the mutated amino acid position (R230) indicated in the C-terminal. (D) The 3-dimensional protein structure indicating wild-type SDHB. (E) The 3-dimensional protein structure showing the mutant SDHB (R230C). (F) The bar diagram displays the LIMBO chaperone binding score of wild-type (score = 3266) and mutant protein of SDHB (score = 3318).

of the C228T *TERT* promoter mutation is likely to have contributed significantly to the rapid progression of PGL.

The association of thyroid cancer with SDHx mutations has rarely been described and whether these mutations play a part in the pathogenesis of PTC or not remains unclear [35–37]. Ni et al screened 375 *PTEN*-negative Cowden syndrome (CS) or Cowden syndrome-like (CSL) patients for *SDHB*, *SDHC*, and *SDHD* mutations [37]. Among these 375 patients, 74 (20%) had increased manganese superoxide dismutase expression, a sign of mitochondrial dysfunction. Among the last group, 10 patients (13.5% of the latter subgroup and 2.7% of the whole group) carried germline mutations in *SDHB* (3/10) or *SDHD* (7/10). No *SDHx* mutations were found in 700 control subjects [37]. The same investigators went on to test these findings in a larger group of 608 *PTEN* mutation-negative CS/CSL patients, of whom 49 (8%)

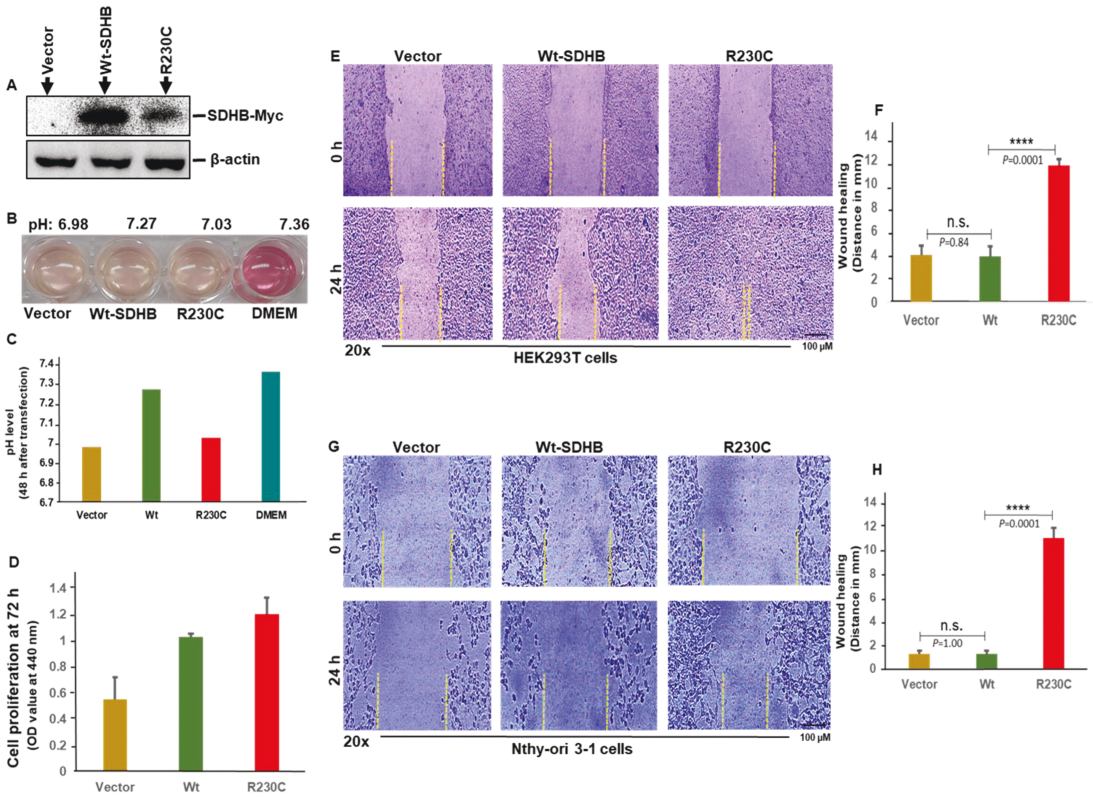

Figure 5. Functional characterization of SDHB (Arg230Cys) mutation. (A) Western blotting analyses of wild-type and mutant SDHB (R230C) expression. HEK293T cells were transiently transfected with Myc-tagged vector, wild-type, and mutant SDHB. Cell lysates from these expression constructs were subjected to Western blotting analyses using appropriate antibodies as indicated in Materials and Methods. (B) A representative illustration shows the color of the cell culture medium collected and photographed after 48 hours from the transiently transfected expression constructs including vector, wild-type SDHB, and mutant SDHB (R230C) with control DMEM. (C). The bar diagram indicates the related pH of the previously indicated various transfected constructs. (D) Cell proliferation of HEK293T cells transfected with SDHB constructs. HEK293T cells were plated in 96-well plate in triplicate 24 hours after transient transfection, maintained in standard condition, and the proliferation assay was performed as described in Materials and Methods. (E) Illustration shows the migrating efficiency of HEK293T cells transiently expressing SDHB constructs in wound healing assay for 0 and 24 hours. (F) Distance of wound healing. The distance of wound healing was calculated and expressed (in millimeters) as the distance of cell coverage to the initial cell-free zone in scratch (0 hours). (G) Illustration shows the migrating efficiency of Nthy-Ori 3-1 cells transiently expressing SDHB constructs in wound healing assay for 0 and 24 hours. These cells were transfected and experimented exactly as indicated earlier for HEK293T cells. (H) Distance of wound healing. The distance of wound healing of Nthy-Ori 3-1 cells was calculated and expressed (×20, in millimeters) as the distance of cell coverage to the initial cell-free zone in scratch (0 hours). Values are presented (panels F, H) as means ± SD of 3 independent experiments. The statistical significance shown as n.s., *, **, ***, and **** indicate not significant, $P < 0.05$, $P < 0.01$, $P > 0.001$, and $P < 0.0001$, respectively, as calculated by unpaired *t* test.

tested positive for germline *SDHx* mutations [38]. They also found *SDHx* mutations in 26 (6%) of 444 *PTEN* mutation-positive CS/CLS patients [38]. The rate of thyroid cancer was significantly much higher in *SDHx* mutation-positive (24/47) patients compared with *PTEN* mutation-positive (27/105, $P = 0.002$) or *PTEN* mutation + *SDHx* mutations-positive patients (6/22, $P = 0.038$) [38]. The authors concluded that *SDHx* mutations are associated with increased risk of malignancy including breast and thyroid cancer in patients with CS/CSL syndromes [38]. Functional studies suggested a crosstalk between PTEN and SDHx, resulting in potentiation of oncogenesis [38]. Papathomas et al studied 3 *SDHB*-mutation- and 3 *SDHD* mutation-positive patients for the occurrence of non-PPGL tumors including 1 PTC in an *SDHD* mutation-positive patient [35]. Although some tumors showed *SDHB*-negative immunohistochemistry results and loss of heterozygosity, PTC and a pituitary adenoma did not show loss of heterozygosity for the germline *SDHD* mutation that the patient had or immunoreactivity for *SDHB* and *SDHA* stains, suggesting no pathogenetic role for the *SDHx* mutations in these cases [35]. All other 3 renal cancers and a pituitary adenoma showed loss of immunoreactivity and heterozygosity. Immunohistochemistry of 348 tumors of different origins, including 60 PTC, was normal with only partial loss of immunoreactivity for SDHB in 2 renal cell cancers [35]. Absence of *SDHx* mutations in the 700 control subjects in the study by Ni et al [38] and the TCGA data [16] and retaining of SDHB and SDHA immunoreactivity in the 348 control subjects in this study [35] all suggest that *SDHx* mutations are rare in sporadic PTC. Although we did not perform *SDHB* immunohistochemistry, the functional studies in HEK293 and Nthy-ori 3-1 thyroid cell line supports its pathogenicity or at least contributes to the pathogenesis of PTC.

The other interesting aspect of our patient is the presence of the well-known *TERT* promotor mutation C228T in PGL, which is a more characteristic mutation of thyroid cancer but was absent in the PTC in our patient. This was not reported in the 184 patients included in the TCGA data for PPGL [4] (Fig. 6). However, it has been reported rarely in PPGL in 2 previous studies. Using Sanger sequencing, Liu et al reported C228T *TERT* promotor mutation in 1 benign PCC and 1 metastatic PGL of 105 PCCs and 13 abdominal PGL examined [39]. In another study, only 2 cases of metastatic extraadrenal PGL (in the urinary bladder) harbored

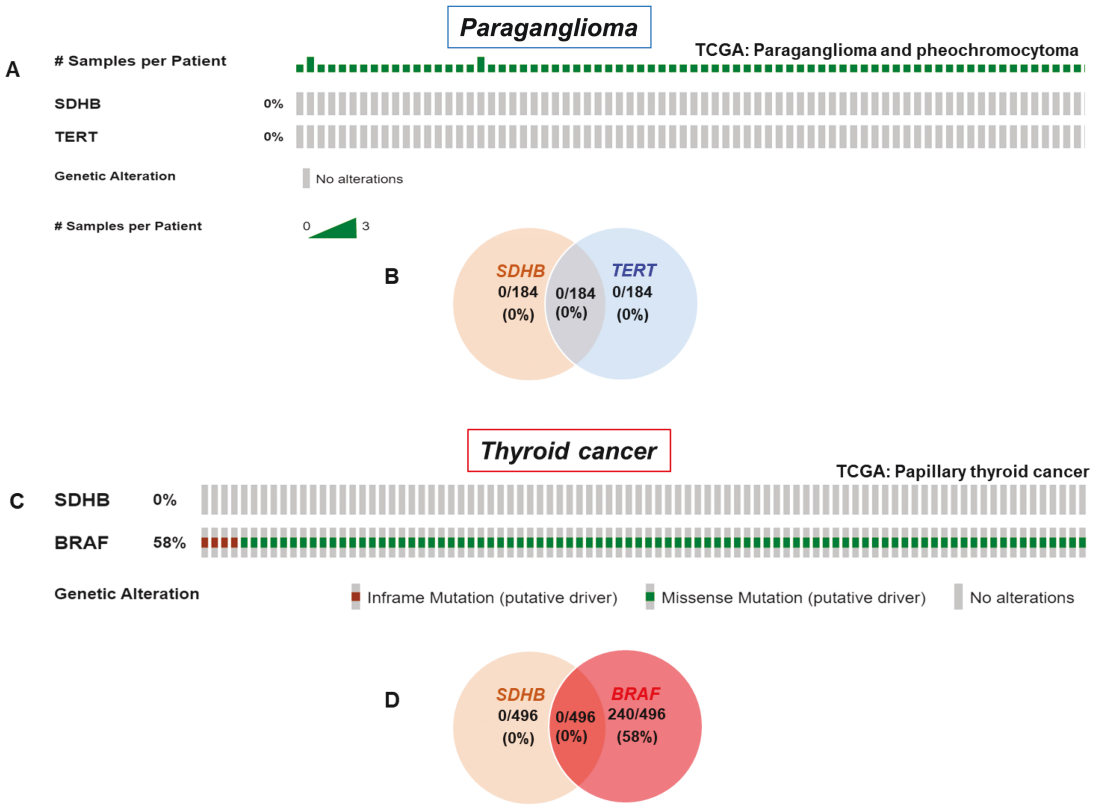

Figure 6. Analyses of the TCGA data for *SDHB* and *TERT* in paraganglioma and *SDHB* and *BRAF* in papillary thyroid cancer. **(**A) The OncoPrint tab shows the *SDHB* and *TERT* gene promoter mutations across the paraganglioma and pheochromocytoma (TCGA). (B) Venn diagram shows the relation between the *SDHB* and *TERT* genes across the TCGA data sets of 184 paraganglioma and pheochromocytoma cases. (C) The OncoPrint tab shows the *SDHB* and *BRAF* gene mutations across the papillary thyroid cancer (TCGA). (D) Venn diagram shows the relation between the *SDHB* and *BRAF* genes across the TCGA data sets of 496 papillary thyroid cancer cases.

the C228T *TERT* promotor mutation out of 127 PCC, 18 abdominal PGL, and 37 head and neck PGL. ATRX is an SWI/SNF chromatin remodelling protein. Similar to the final outcome of TERT, ATRX mutations contribute to telomere length maintenance by promoting alternative lengthening of telomeres. *ATRX* mutations have been found in 4 cases in PPGL TCGA data and in 12.6% of 103 PPGL in another study [40] and were clearly associated with more aggressive tumors [40]. In a recent study of 200 PPGL, different mechanisms of telomerase activation were investigated [41] for *TERT* promotor mutations and other mechanisms of telomerase activation [41]. One *SDHC*-mutated benign tumor, 1 metastatic *SDHC*-mutated PGL, and 5 *SDHB*-mutated metastatic tumors carried the C228T mutation [41]. In the same study, *ATRX* mutations were found in 8 PPGL (4%), mostly in *SDHx* mutation-positive patients and one-half of them have metastatic PPGL [41].

In conclusion, we presented a patient in whom an *SDHB* mutation predisposed to the development of an abdominal PGL harboring a somatic *TERT* promotor mutation that likely potentiated the aggressiveness of the PGL and leading to progressive distant metastases. This suggests that, in addition to the primary underlying germline mutations, other genetic and epigenetic alterations may contribute to the development and progression of distant metastases in PGL. The *SDHB* mutation may have also contributed to the initiation steps and progression of PTC along with the somatic $BRAF^{V600E}$ mutation. However, this remains speculative because it is hard to make a definite conclusion based on 1 case and with no experimental work was performed to support that. Further studies to determine the prevalence of SDHx mutations in PTC and its exact contribution to its pathogenesis are needed. In the current case, it is possible that the cooccurrence of PTC in this patient with *SDHB*-induced PGL was a coincident because PTC is quite common and *SDHB* mutations are rare.

Acknowledgments

We thank Dr. Yufei Shi for providing us with cells and the members of the Department of Molecular Oncology for their support.

Funding

The was no specific funding for this work.

Conflict of Interest

The authors have no conflicts of interest to declare.

Data Availability

All data generated or analyzed during this study are included in this published article.

References

1. Lenders JW, Duh Q-Y, Eisenhofer G, *et al*. Pheochromocytoma and paraganglioma: an Endocrine Society clinical practice guideline. *J Clin Endocrinol Metab*. 2014;99(6):1915-1942.

2. Neumann HP, Young WF, Jr, Eng C. Pheochromocytoma and paraganglioma. *N Engl J Med*. 2019;381(6):552-565. doi:10.1056/nejmra1806651.
3. Erickson D, Kudva YC, Ebersold MJ, *et al*. Benign paragangliomas: clinical presentation and treatment outcomes in 236 patients. *J Clin Endocrinol Metab*. 2001;86(11):5210-5216.
4. Fishbein L, Leshchiner I, Walter V, *et al*; Cancer Genome Atlas Research Network. Comprehensive molecular characterization of pheochromocytoma and paraganglioma. *Cancer Cell*. 2017;31(2):181-193. doi:10.1016/j.ccell.2017.01.001.
5. Pang Y, Liu Y, Pacak K, Yang C. Pheochromocytomas and paragangliomas: from genetic diversity to targeted therapies. *Cancers*. 2019;11(4):436. doi:10.3390/cancers11040436.
6. Flores SK, Estrada-Zuniga CM, Thallapureddy K, Armaiz-Peña G, Dahia PLM. Insights into mechanisms of pheochromocytomas and paragangliomas driven by known or new genetic drivers. *Cancers*. 2021;13(18):4602. doi:10.3390/cancers13184602.
7. Buffet A, Burnichon N, Favier J, Gimenez-Roqueplo A-P. An overview of 20 years of genetic studies in pheochromocytoma and paraganglioma. *Best Pract. Res. Clin. Endocrinol. Metab*. 2020;34(2):101416. doi:10.1016/j.beem.2020.101416.
8. Nölting S, Bechmann N, Taieb D, Beuschlein F, Fassnacht M, Kroiss M, Eisenhofer G, Grossman A, Pacak K. Personalized management of pheochromocytoma and paraganglioma. *Endocrine Reviews*. 2021;43(2):199-239.
9. Gimenez-Roqueplo AP, Favier J, Rustin P, *et al*. Mutations in the SDHB gene are associated with extra-adrenal and/or malignant phaeochromocytomas. *Cancer Res*. 2003;63(17):5615-5621.
10. van Hulsteijn LT, Dekkers OM, Hes FJ, Smit JW, Corssmit EP. Risk of malignant paraganglioma in SDHB-mutation and SDHD-mutation carriers: a systematic review and meta-analysis. *J Med Genet*. 2012;49(12):768-776.
11. Seib CD, Sosa JA. Evolving understanding of the epidemiology of thyroid cancer. *Endocrinol Metab Clin North Am*. 2019;48(1):23-35.
12. Tuttle RM, Alzahrani AS. Risk stratification in differentiated thyroid cancer: from detection to final follow-up. *J Clin Endocrinol Metab*. 2019;104(9):4087-4100.
13. Haugen BR. 2015. American thyroid association management guidelines for adult patients with thyroid nodules and differentiated thyroid cancer: what is new and what has changed? *Cancer*. 2017;123(3):372-381.
14. Tuttle RM, Tala H, Shah J, *et al*. Estimating risk of recurrence in differentiated thyroid cancer after total thyroidectomy and radioactive iodine remnant ablation: using response to therapy variables to modify the initial risk estimates predicted by the new American Thyroid Association staging system. *Thyroid*. 2010;20(12):1341-1349.
15. Yan KL, Li S, Tseng C-H, Kim J, Nguyen DT, Dawood NB, Livhits MJ, Yeh MW, Leung AM. Rising incidence and incidence-based mortality of thyroid cancer in California, 2000-2017. *Journal Clinical Endocrinology & Metabolism*. 2020;105(6):1770-1777.
16. Cancer Genome Atlas Research N. Integrated genomic characterization of papillary thyroid carcinoma. *Cell*. 2014;159(3):676-690.
17. Pak K, Suh S, Kim SJ, Kim IJ. Prognostic value of genetic mutations in thyroid cancer: a meta-analysis. *Thyroid: Official J Am Thyroid Assoc*. 2015;25(1):63-70.
18. Xing M. BRAF mutation in thyroid cancer. *Endocr Relat Cancer*. 2005;12(2):245-262. doi:10.1677/erc.1.0978.
19. Xing M, Alzahrani AS, Carson KA, *et al*. Association between BRAF V600E mutation and mortality in patients with papillary thyroid cancer. *Jama*. 2013;309(14):1493-1501.
20. Xing M, Alzahrani AS, Carson KA, *et al*. Association between BRAF V600E mutation and recurrence of papillary thyroid cancer. *J Clin Oncol*. 2015;33(1):42-50. doi:10.1200/JCO.2014.56.8253.
21. Liu R, Xing M. TERT promoter mutations in thyroid cancer. *Endocr Relat Cancer*. 2016;23(3):R143-R155. doi:10.1530/ERC-15-0533.
22. Landa I, Ganly I, Chan TA, *et al*. Frequent somatic TERT promoter mutations in thyroid cancer: higher prevalence in advanced forms of the disease. *J Clin Endocrinol Metab*. 2013;98(9):E1562-E1566.
23. Ren H, Shen Y, Hu D, He W, Zhou J, Cao Y, Mao Y, Dou Y, Xiong W, Xiao Q, Zhang Y, Su X. Co-existence of BRAF(V600E) and TERT promoter mutations in papillary thyroid carcinoma is associated with tumor aggressiveness, but not with lymph node metastasis. *Cancer Manag Res*. 2018;10:1005-1013.
24. Alzahrani AS, Alsaadi R, Murugan AK, Sadiq BB. TERT promoter mutations in thyroid cancer. *Horm Cancer*. 2016;7(3):165-177. doi:10.1007/s12672-016-0256-3.
25. Panebianco F, Nikitski AV, Nikiforova MN, Nikiforov YE. Spectrum of TERT promoter mutations and mechanisms of activation in thyroid cancer. *Cancer Med*. 2019;8(13):5831-5839. doi:10.1002/cam4.2467.
26. Astuti D, Latif F, Dallol A, *et al*. Gene mutations in the succinate dehydrogenase subunit SDHB cause susceptibility to familial pheochromocytoma and to familial paraganglioma. *Am J Hum Genet*. 2001;69(1):49-54. doi:10.1086/321282.
27. Cohen Y, Xing M, Mambo E, *et al*. BRAF mutation in papillary thyroid carcinoma. *J Natl Cancer Inst*. 2003;95(8):625-627. doi:10.1093/jnci/95.8.625.
28. Liu X, Bishop J, Shan Y, *et al*. Highly prevalent TERT promoter mutations in aggressive thyroid cancers. *Endocr Relat Cancer*. 2013;20(4):603-610.
29. Tseng PL, Wu WH, Hu TH, *et al*. Decreased succinate dehydrogenase B in human hepatocellular carcinoma accelerates tumor malignancy by inducing the Warburg effect. *Sci Rep*. 2018;8(1):3081. doi:10.1038/s41598-018-21361-6.
30. Murugan AK, Liu R, Xing M. Identification and characterization of two novel oncogenic mTOR mutations. *Oncogene*. 2019;38(26):5211-5226. doi:10.1038/s41388-019-0787-5.
31. Murugan AK, Al-Amr A, Al-Ansari MM, Manogaran PS, Al-Hindi H, Alzahrani AS. Single nucleotide polymorphisms in matrix metalloproteinase 2 (MMP2) enhance BRAFV600E mutation-mediated oncogenicity and invasiveness of papillary thyroid cancer cells. *Endocr Relat Cancer*. 2021;28(4):273-289.
32. Murugan AK, Ihara S, Tokuda E, Uematsu K, Tsuchida N, Fukui Y. SWAP-70 is important for invasive phenotypes of mouse embryo fibroblasts transformed by v-Src. *IUBMB Life*. 2008;60(4):236-240. doi:10.1002/iub.33.
33. Gao J, Aksoy BA, Dogrusoz U, *et al*. Integrative analysis of complex cancer genomics and clinical profiles using the cBioPortal. *Sci Signal*. 2013;6(269):pl1.
34. Yang C, Matro JC, Huntoon KM, *et al*. Missense mutations in the human SDHB gene increase protein degradation without altering intrinsic enzymatic function. *FASEB J*. 2012;26(11):4506-4516.
35. Papathomas TG, Gaal J, Corssmit EP, *et al*. Non-pheochromocytoma (PCC)/paraganglioma (PGL) tumors in patients with succinate dehydrogenase-related PCC-PGL syndromes: a clinicopathological and molecular analysis. *Eur J Endocrinol*. 2014;170(1):1-12.
36. Wolf KI, Jacobs MF, Mehra R, *et al*. A family with a carotid body paraganglioma and thyroid neoplasias with a new SDHAF2 germline variant. *J Endocr Soc*. 2019;3(11):2151-2157.
37. Ni Y, Zbuk KM, Sadler T, *et al*. Germline mutations and variants in the succinate dehydrogenase genes in Cowden and Cowden-like syndromes. *Am J Hum Genet*. 2008;83(2):261-268.
38. Ni Y, He X, Chen J, *et al*. Germline SDHx variants modify breast and thyroid cancer risks in Cowden and Cowden-like syndrome via FAD/NAD-dependant destabilization of p53. *Hum Mol Genet*. 2012;21(2):300-310.
39. Liu T, Brown TC, Juhlin CC, *et al*. The activating TERT promoter mutation C228T is recurrent in subsets of adrenal tumors. *Endocr Relat Cancer*. 2014;21(3):427-434.
40. Fishbein L, Khare S, Wubbenhorst B, DeSloover D, D'Andrea K, Merrill S, Cho NW, Greenberg RA, Else T, Montone K, LiVolsi V, Fraker D, Daber R, Cohen DL, Nathanson KL. Whole-exome sequencing identifies somatic ATRX mutations in pheochromocytomas and paragangliomas. *Nat Commun*. 2015;6:6140.
41. Job S, Draskovic I, Burnichon N, *et al*. Telomerase activation and ATRX mutations are independent risk factors for metastatic pheochromocytoma and paraganglioma. *Clin Cancer Res*. 2019;25(2):760-770.